A Molecular Probe of Dark Energy

Rodger I. Thompson[1], Jill Bechtold[1], Daniel Eisenstein[1], Xiaohui Fan[1], Robert Kennicutt[1,2] and Carlos Martins[2,3]

1) Steward Observatory, University of Arizona, 2) Cambridge University, 3) CFP, University of Porto

Overview of Goals and Techniques

Numerous theories of dark energy invoke evolving scalar fields, "e.g. quintessence" that lead to time and possibly spatial variations in the fundamental constants (rolling constants). We propose to accurately constrain or detect variations in the ratio of electron to proton mass, $\mu = m_e/m_p$, by observing the Lyman and Werner rest frame UV absorption lines of molecular hydrogen in the spectra of QSOs whose sight lines intersect Damped Lyman Absorbers (DLAs) that have a high abundance of H_2. Molecular spectra are particularly sensitive to changes in μ since their rotational, vibrational, and electronic energy levels are proportional to μ, $\sqrt{\mu}$, and the reduced mass of μ respectively, so that each absorption line has a unique and *different* shift for a given $\Delta\mu$. The H_2 Lyman and Werner bands have many absorption lines *from the same lower state* to monitor shifts in identical spatial and velocity components of the absorbing gas. Uncertainty due to isotopic composition is not relevant for H_2 since the wavelengths shifts in the next isotopic state, HD, are orders of magnitude larger than the expected shifts due to a $\Delta\mu$. The current best constraint on $\Delta\mu$ is $\Delta\mu/\mu = -0.5 \pm 3.6\times10^{-5}$ (Ubachs & Reinhold 2004). The program produces limits on $\Delta\mu/\mu$ of 10^{-5} utilizing current instrumentation and $\Delta\mu/\mu \le 10^{-6}$ with a dedicated facility. An accurate limit on $\Delta\mu$ not only constrains quintessence theories of dark energy but also Grand Unification Theories (GUTs), particularly when coupled with equivalent constraints on the change of the fine structure constant α with time.

Brief Description of the Baseline Program

The program has three stages. The first is to take high resolution (R = 80,000) spectra with existing facilities of QSOs known to have molecular hydrogen absorption lines to search for changes in μ. The observations are optimized for accurate wavelength determination and analysis techniques are optimized for placing limits on or detecting $\Delta\mu$.

The second stage of the program is the construction of a very efficient, high resolution spectrometer for the observation of point objects. The expected resolution of the spectrometer is $R=10^6$ and it is designed to push the limits on $\Delta\mu$ to at least 10^{-6}. A candidate telescope for the spectrometer is the Large Binocular Telescope (LBT) on Mt. Graham in Arizona, but other facilities are also considered.

The third stage of the program recognizes that the time available on a multi-purpose, multi-institution telescope is necessarily limited and that a dedicated facility, the μ machine, is required for pushing past $\Delta\mu = 10^{-6}$. The μ machine is a dedicated 8-10m telescope and spectrometer, optimally designed for pursuing rolling μ *and* α to constrain not only theories of dark energy but also high energy unification theories. If part one is particularly successful it may be more expedient to proceed directly to part 3 where the telescope and spectrometer can be optimized as a system.

Introduction

A range of observational data sets suggest that the universe is currently dominated by a dark energy component whose gravitational behavior is very similar to that of a cosmological constant. This could of course be due to a cosmological constant, but the value required by observations is so much lower than predicted by particle physics theories that many believe a dynamical scalar field is a more likely candidate. Specifically, motivation for this comes from superstring models, where any dimensionful parameter is expressed in terms of the string mass scale and a scalar field vacuum expectation value. The requirements of slow-roll (which is mandatory for $p<0$) and present-day domination imply, if the minimum of the potential is zero, that the field excitations must be very light, $m \approx H_0 \approx 10^{-33}$ eV while today the field is of order m_{Planck}.

Crucially, couplings of this field lead to observable long-range forces and spacetime variation of fundamental coupling constants, even in late cosmology. Provided no symmetry cancels it, there is a term in the effective Lagrangian coupling baryonic matter to the scalar field. As the field evolves over cosmological time scales, such couplings lead to a time dependence of the coupling constants of baryonic matter. Bounds on the time variation of constants therefore restrict the evolution of the scalar field, and thereby provide constraints on dark energy that are complementary to those obtained by more traditional means (e.g., CMB, LSS surveys, supernovae).

We propose to improve the quality of the spectroscopic constraints on $\Delta\mu/\mu$ to provide a unique tool to discriminate between competing dark energy models. Indeed, given any possible form for the evolution of the equation of state of the universe with redshift, $w(z)$, there is a quintessence model that will reproduce it exactly, as can be seen by inverting the Friedmann and Raychaudhuri equations. Similarly, given any possible form of the variation of the couplings with redshift $\mu(z)$ or $\alpha(z)$ there is a model that reproduces them exactly. However, the crucial point is that for a given model, the redshift dependencies of the couplings and w are related in a unique way. In other words, if one chooses a particular dark energy model (or class of models) and uses observations of $w(z)$ to calibrate its free parameters, one can in principle derive an unambiguous prediction for $\mu(z)$ and $\alpha(z)$ that can be subsequently tested. By probing the redshift evolution of $w(z)$, $\alpha(z)$ and $\mu(z)$ we can in principle test GUT scenarios without needing to detect any grand-unified model particles in accelerators.

These studies are made particularly interesting by the wide range of possible relations between μ and α and their respective cosmological evolutions. Indeed, there is so much model dependence that not even the relative sign of the variations is generically fixed, although each particular model will yield a specific prediction for this relation. To take a specific example, we focus on the minimal supersymmetric standard model, embedded on a grand unified theory. Then the relations between α, μ and the QCD scale Λ that will have the form $\frac{\dot{\mu}}{\mu} \approx \frac{\dot{\Lambda}}{\Lambda} \approx \Re\frac{\dot{\alpha}}{\alpha}$ If the variation of α is due to a time variation of the corresponding unified coupling constant, then $\Re$ will be positive and typically $\Re \approx 40$, whereas if the variation is due to a time variation of the grand unification scale then $\Re$ will be negative, with a comparable magnitude. So in the former case the time variations of α and μ will have the same sign, but in the latter they will have opposite signs. It is clear therefore that the proposed studies to constrain $\Delta\mu$ are a powerful tool to constrain theories of dark energy. A more powerful constraint on $\Delta\mu$ limits the range of dark energy theories and strengthens the case for a cosmological constant while a detection of a variation in μ points toward a scalar field as a major component of dark energy. Either case has a profound effect on our understanding of the universe.

Relevant Astrophysics

The spectra of distant QSOs show many absorption lines of atomic hydrogen produced by cold gas clouds along the line of sight to the QSO. The system of absorption lines is called the Lyman forest and has been the subject of intensive study. Some of these spectra also show absorption lines from molecular hydrogen from cold molecular clouds along the line of sight. The absorption lines are from the ground electric and vibrational state to the first two excited electronic states called the Lyman and Werner bands respectively. Since the molecular gas is very cold only the first few rotational states of the lower state are populated, however, there are many absorption lines for each rotational level to the vibrational and rotational levels of the two electronic upper states as is shown in Figure 1 and 2. Their rest wavelength is ~1000 angstroms which is then red-shifted to the visible spectral region where they can be observed from the ground.

Relevant Molecular Physics

It has long been known (Born & Oppenheimer 1927) that the energy levels of molecules can be expanded in powers of $\rho = \sqrt{m_e/m_p} = \sqrt{\mu}$. Note that μ is the symbol of common choice to denote m_e/m_p even though it can be confused with the reduced mass or the magneton. The literature is also equally split between the electron to proton mass ratio and the proton to electron mass ratio. We use m_e/m_p as it is the natural unit in the expansion of molecular energies. Thompson (1975) first pointed out that the dependence on μ provided a method for constraining the evolution of μ through molecular spectra observed at high redshift. To first order the rotational energy is proportion to ρ^2 and the vibrational energy is proportional to ρ. The vibrational energy levels $G(\nu)$, where ν is the vibrational quantum number, are given by

$$G(\nu) = \rho\omega_e\left(\nu+\frac{1}{2}\right) - \rho^2\omega_e x_e\left(\nu+\frac{1}{2}\right)^2 + \rho^3\omega_e y_e\left(\nu+\frac{1}{2}\right)^3 + \ldots \quad (1$$

and the rotational energy is given by

$$F(J) = \rho^2\left(B_e - \rho\alpha_e\left(\nu+\frac{1}{2}\right)\right)J(J+1) - \rho^4\left(D_e - \rho\beta_e\left(\nu+\frac{1}{2}\right)\right)J^2(J+1)^2 + \ldots \quad (2$$

where J is the rotational quantum number and the other quantities are the molecular constants specific to H_2. The molecular constants are in units where $\mu = 1$. The ground state and first two electronic states are shown in Figure 2 with the $X\ ^1\Sigma_g^+$ - $B\ ^1\Sigma_u^+$ Lyman band on the left and the $X\ ^1\Sigma_g^+$ - $C\ ^1\Pi_u$ Werner band on the right. Eq. (1 and (2 provide the means of computing the shift of each line as a function of $\Delta\mu$. This is usually expressed as a sensitivity constant, K_i, for each transition i where K_i is defined by

$$\lambda_i = \lambda^0{}_i(1+z_{abs})\left(1+K_i\frac{\Delta\mu}{\mu}\right) \quad (3$$

Calculations for the H_2 molecule, based on the description of energy levels discussed above, give K_i that range from -0.007 to 0.058 for observed H_2 absorption lines (Varshalovich & Potekhin 1995, Potekhin et al. 1998). Table 1 gives the K_i for a few observed Lyman and Werner lines.

μ, α, and Radio Measurements

The program for constraints on μ is complimentary to programs that measure constraints on α and radio observations relevant to μ, but it also offers significant advantages. A problem that

affects measurement of $\Delta\alpha$ at optical wavelengths and $\Delta\mu$ from radio observations is that the observations compare line shifts from different atoms, ionization states, or excitations of molecules. This often means that the measurements come from different components of the absorbing gas that may have different velocities. H_2 on the other hand, as shown in Figure 2 has many lines of different shifts that arise from the same lower state, insuring that they all come from the same gas, eliminating errors due to differential velocities. Although the radio observations of CO have very high frequency accuracy, they compare lines from different excitation lower states and are limited by the internal dynamics of the absorbers. The H_2 measurements are also immune to contamination by other isotopic species since the shift in the next isotopic molecule, HD, is accurately known and orders of magnitude larger than the expected shift due to a $\Delta\mu$. The small isotopic shift in the atomic spectra searching for changes in α may be a limiting factor in accuracy (Ashenfelter, Mathews and Olive 2004). A very important feature of the H_2 is that the $\Delta\mu$ shift of each line is different, therefore redshift errors can not mimic the effect of $\Delta\mu$. This is a trait shared by the $\Delta\alpha$ measurements but they involve different atomic species and ions and are therefore subject to the gas dynamics as discussed above. A theoretical advantage, discussed in the introduction, is that the expected change in μ is about 40 times that of α. Given the possible range of theoretical models this is only a modest advantage. The best progress, however is made when all of the constraints on fundamental constants are considered as an ensemble.

Observational Parameters

The achievable constraints on $\Delta\mu$ depend on both the resolution and signal to noise of the observed spectrum. The following gives the dependence of $\Delta\mu$ on these quantities.

$\Delta\mu$ as a Function of R

The resolution R of a spectrometer is defined as $\lambda/\Delta\lambda$ where $\Delta\lambda$ is the wavelength increment spanned by two adjacent pixels. An observational "rule of thumb" is that a line center can be determined to approximately 1/10 of a pixel using the normal emission calibration source observed at regular intervals and 1/50 of a pixel when a calibration source such as an Iodine absorption cell is used to produce absorption lines along the identical optical path as the astronomical light (Marcy & Butler 1992). This gives a wavelength precision of 1/(100R). As an example consider two transitions from Table 1, L(1-0)R(0) and L(9-0)R(0) that have identical ground states. Using the K_i in Table 1 and Eq. (3 we find a shift between the lines of $\Delta\lambda/\lambda = 3.26\times10^{-2}\Delta\mu/\mu$. Equating that to the line center accuracy we find

$$\Delta\mu/\mu = 0.3/R \qquad (4$$

which gives $\Delta\mu = 4 \times 10^{-6}$ for R = 80,000. Taking advantage of the many pairs of lines and the line set as an ensemble improves the accuracy of the measurement and provides important checks on the results. In the absence of quantitative measures of the improvements from the ensemble matching and taking with caution the ability to determine line centers to 1/50 of a pixel we will leave the expected $\Delta\mu$ determination for R = 80,000 at the value above. Marcy and Butler (1992), however, have achieved velocity accuracy higher than this with an R = 40,000 spectrometer. In the case of H_2 lines the Lyman forest lines offer the same advantage as the absorption cell, offering many lines of known wavelength to provide the accurate *relative* wavelength calibration. Since each H_2 line has a different shift with $\Delta\mu$ we are only interested in the relative shift of the lines with respect to each other and not on their absolute redshift.

Sensitivity to Achieve R

A second rule of thumb is that to achieve the above accuracy in line centers a signal to noise in each pixel of approximately 30 is required which is about 1000 counts per pixel. For this calculation we will assume the HIRES spectrometer on the Keck telescope as the baseline although the UVES spectrometer on the VLT might be slightly more sensitive but less accessible to US observers. The 5000 Angstrom photon flux of an object of magnitude m for the Keck telescope is approximately $f = eff\frac{2\times10^{12}}{R}10^{\frac{-m}{2.5}}$ photons per second where *eff* is the efficiency of the total system of sky, telescope and spectrometer. The efficiency of the HIRES spectrometer alone is shown in Figure 3 If we assume that atmospheric transmission, the telescope, and slit efficiency is 30% we get a total efficiency of 0.03. We can then express the time to achieve 1000 photons total signal in each pixel at resolution R as

$$t = 1.7\times10^{-8}R10^{\frac{m}{2.5}} \quad (5$$

For R = 80,000 t is equal to 10^4 seconds at a magnitude of 17.2. This means that the QSOs with known H_2 absorption lines can be observed with total integration times of a few x 10^4 seconds.

Precursor Observations

Table 2: shows the 9 known DLA systems with H_2 absorption. Although these systems are enough to determine stringent limits on the variation of μ at large redshift it is useful to have more systems over a range of redshifts, particularly if a variation in μ is found. Eight of these systems were found in a survey by Ledoux, Petitjean, & Srianand (2003) who surveyed 33 candidates and found H_2 in 8 of them. The common factor in the H_2 systems was a high metallicity and high depletion of Fe, probably into grains where H_2 can form. The expected 100,000 SDSS QSO spectra are expected to yield ~2000 DLAs, with H_2 in approximately 5-10%. This yields ~30 sources with the appropriate redshift and magnitude for high resolution spectroscopy.

Although not needed for the first set of observations, precursor laboratory work will be required to utilize very high resolution spectra of H_2. Ubachs & Reinhold (2004) have recently improved the laboratory measurements of the H_2 wavelengths to an accuracy of 5×10^{-8} which is now more accurate than the present astronomical wavelength precision. Further improvement to 1×10^{-8} is required to improve limits of $\Delta\mu/\mu$ to 10^{-6} given the factor ~100 difference between wavelength accuracy and μ accuracy.

First Stage: Observations with Existing Facilities

We will use the R=80,000 HIRES observations discussed above as the reference point for the use of existing facilities with essentially similar performance for the blue arm of the UVES on the VLT. The calculations above show that, taking into account efficiency and weather factors, we can expect to achieve approximately one spectrum with appropriate signal to noise per night of observation. We will take high resolution spectra at the Keck or VLT telescopes of the three high redshift known QSO H_2 systems, Q0347-383, Q0405-443, and Q0528-250. The latter is observable with Keck while the first two are optimally suited for the VLT. These spectra form the base-

line for the development of specialized techniques for analyzing spectra to produce the best constraints on $\Delta\mu$.

Line Pairings

One technique that will be investigated is the concept of line pairing. The existence of the Werner bands at a higher electronic upper level superimposes lines with a small or even negative K factor very near in wavelength to Lyman lines with a large positive K factor. The Lyman line will also have a companion line, R, or P (for J >0) also at a very similar wavelength and with a very similar K factor as the original Lyman line while the Werner line will have two companion lines of R, Q, or P. The spacings between the two lines in the same band will be essentially determined by the redshift while the spacing between the lines in the two different bands will be determined by the redshift and any change in μ. These pairings are self calibrating and since they are within a few angstroms of each other, they are relatively immune to distortions in the wavelength solution. An excellent example of this is the L(7-0) and W(0-0) transitions with rest wavelengths within 3 angstroms of each other. There are many such pairings so that the probability of observing a set of lines with minimal Lyman forest contamination is relatively high. Future instruments may focus on these pairings rather than trying to cover a broadband of wavelengths.

Second Stage: Optimized Spectrometer for Existing Telescopes

Inspection of Figure 1 indicates that HIRES is at best 10% efficient in its highest efficiency wavelength region which reduces to 3% or less when high resolution slit and other losses are taken into account. This is typical for general user, multiple use spectrometers where many possible observing modes must be accommodated. This leads to the possibility of a optimized spectrometer for highly efficient, high spectral resolution observations of point sources. The goal is a R=100,000-500,000 spectrometer for point sources with a total efficiency of 50%. This is achievable with current technology. The high efficiency reduces observing times by almost a factor of 100 compared to present spectrometers at the same resolution. The spectrometer is temperature controlled and installed at a permanent location such as the Nasmith focus of the Large Binocular Telescope or a similar facility.

Third Stage: Optimized Spectrometer/Telescope - The μ Machine

Although progress can be made with the current generation of telescopes the basic problem with multi-use telescopes is obtaining sufficient time to achieve the spectral resolution and signal to noise needed to put strong limits on the variation in μ. The best attack on the question of varying μ is a dedicated facility, the μ machine, that is optimized as a system for precise measurement of molecular hydrogen absorption lines in the spectra of QSOs.

The μ machine is a 8-10 meter telescope which feeds approximately 4 different spectrometers. Each spectrometer is optimized for a particular wavelength region with spectral resolutions of R = 10^6. The spectrometers are permanently installed at the Nasmith focus of the telescope. There is no need for wide fields of view since we are observing point objects. The spectra gathered by the μ machine are also useful for placing constraints on the time evolution of the fine structure constant α. Bright time observations of galactic stars contributes to the detailed study of nucleosynthesis as a side benefit for efficient use of the facility.

The goal of the μ machine is a complete system efficiency of 50% at a resolution of $R=10^6$. As an example of its capabilities presuming a 10m telescope, an 18th magnitude source at 5000 Angstroms produces 0.065 detected photons per second per pixel assuming 2 pixels per resolution element. In 1600 seconds 100 counts are collected which makes the photon noise dominant over the read noise of present day detectors. The new HIVISI silicon detectors from the Rockwell Scientific Company with non-destructive reads can reject any cosmic ray hits that occur within that period. A signal of 1000 counts is achieved in 16,000 seconds for high signal to noise and accuracy. Therefore, the μ machine achieves $R=10^6$ spectra in the same time as current facilities achieve R=80,000 Wavelength calibration with possibly appropriate absorption cells and the Lyman forest establishes line positions to 1/50 of a pixel which gives a line position to 1 part in 10^8. As an example, using the K factors listed in Table 1, the Lyman (9-0)R(0) line produces a shift of 4 times this amount for a fractional shift in μ of 10^{-6}. The combination of the typical 10-20 isolated H_2 lines produces an accuracy of 3 to 4 times this amount. At these accuracies a comparable increase in the laboratory measurements is needed. If μ is found to be a rolling constant then many QSO/DLA systems in many parts of the sky and at differing redshifts must be observed to check for spatial variations and the functional dependence on z. Only a dedicated facility is capable of that extensive program.

Error Budget

The primary sources of error in measuring $\Delta\mu/\mu$ are errors in the observed wavelengths, errors in the measured rest frame wavelengths, and errors in the measured molecular constants used in predicting the shifts. The best available laboratory wavelengths of the H_2 Lyman and Werner bands are from Ubachs and Reinhold (2004) at an accuracy of 5×10^{-8} although they speculate that the accuracy is actually greater than that. The shifts for a $\Delta\mu/\mu$ of 10^{-6} are of the same order therefore the present day laboratory data will contribute a significant error to the investigation. Part of a comprehensive $\Delta\mu$ search is an improvement in the laboratory measurements. Observed wavelength errors have many sources as are described in Murphy et al. (2003). A set of dedicated spectrometers, as described above, will mitigate several of these but utmost care will be needed to control the errors. The large range of K factors for the different transitions greatly reduces the effect of systematic errors. The K factors increase with vibrational quantum number as does the frequency of the transition. This is offset by the mixing of low vibrational number Werner transitions with the Lyman bands. As an example the Lyman (9-0)R(0) band transitions has a rest wavelength only 2.3 Angstroms shorter than the Werner (0-0)P(3) transition.

A strong source of wavelength error is the blending of atomic hydrogen Lyman forest lines with the H_2 lines. The QSO lines of sight generally only intercept one DLA with molecular hydrogen but intercepts many more DLAs with only atomic material. These additional DLAs produce a random distribution of lines on top of the molecular lines. Since all of the lines are very narrow, high spectral resolution helps with this error source. In practice the already observed systems have 10 to 20 isolated lines at resolutions of a few times 10^4. The proposed 10^6 resolution of the new spectrometers greatly increases that number and decreases the chance of blended lines as an error source.

Another source of wavelength error is differential velocity components. This is particularly true when transitions occur in different species or in different ground energy states of the same

species. The large number of transitions from the same ground state in molecular hydrogen mitigates this error source. The analysis is done independently for each rotational lower state of H_2 to insure that the lines arise from the same gas component of the DLA.

Risks and Strengths

An outstanding strength of this investigation is that both positive and negative results have a strong influence on theories of dark energy. Measurement of a change in μ with time will both validate and constrain theories that go beyond the standard model of particle physics while a strong limit on any change in μ provides strong limits on theories of dark energy that require changes in fundamental constants with time.

Technology Development

The initial part of the program that utilizes existing facilities does not require any technology development. Pursuit of a high precision, very efficient spectrometer for observing point sources does not require any new technology but careful execution and implementation of existing technology. A complete systems approach dedicated to extremely high throughput must be rigidly employed. The construction of the μ machine itself, although more expensive, does not involve any new technology as large telescopes have been built. It is actually less demanding than the high throughput spectrometer that has to be matched to existing telescopes as opposed to the telescope/spectrometer μ machine that can be designed as a system.

Timeline

Fall 2006 -- VLT/Keck observations
2007 -- Start of Spectrometer Design and Construction
2009 -- Start of μ Machine Design
2011-- Commissioning of Spectrometer on LBT
2011 -- Start of μ Machine Construction
2011 - 2016 -- Observations with Spectrometer
2016 -- Commissioning of μ Machine
2016 -- Observations with μ Machine

References

Ashenfelter, T.P., Mathews, G.J., & Olive 2004, Ap.J., 615, 82.
Born, M., & Oppenheimer, J.R. 1927, Ann. Physik, 84, 457
Ivanchik, A. et al. 2003, Astrophysics and Space Science, 283, 583
Ledoux, C., Petitjean, P. & Srianand, R. 2003, MNRAS, 346, 209
Marcy, G. W. & Butler, R. P. 1992, PASP, 104, 270
Murphy, M.T., Webb, J.K., & Flambaum, V.V. 2003, MNRAS, 345, 609
Potekhin, A.Y. et al. 1998, Ap.J., 505, 523
Thompson, R.I., 1975, Astrophysical Letters, 16, 3
Ubachs, W. & Reinhold, E. 2004, Phys. Rev. Let., 92, 101302
Varshalovich, D.A. & Potekhin, A.Y. 1995, Space Science Reviews, 74, 259

Tables

Table 1: Isolated H_2 Lines Observed in Q0528-250 and Q0347-382

Transition[a]	Rest Wavelength[b] Angstroms	K Factor ($x10^{-3}$)[c]
L(0-0)R(1)	1108.633	-7.19
L(0-0)P(1)	1110.062	-8.44
W(0-0)Q(2)	1010.9389	-6.86
L(1-0)R(0)	1092.194	-0.55
L(1-0)R(1)	1092.732	-1.07
L(1-0)P(1)	1094.051	-2.21
L(2-0)R(0)	1077.13874*	5.08
W(2-0)Q(1)	966.0937	14.23
L(2-0)R(1)	1077.698	4.53
L(2-0)R(3)	1081.265	1.33
L(2-0)P(3)	1084.5618	-0.98
L(3-0)P(1)	1064.60539*	8.65
L(3-0)R(3)	1067.4738	7.58
W(3-0)Q(1)	947.4218	21.76
W(3-0)P(3)	951.6722	17.24
L(4-0)R(0)	1049.36744*	14.9
L(4-0)R(1)	1049.95976	14.3
L(4-0)P(1)	1051.03253*	13.4
L(4-0)R(2)	1051.49858*	12.8
L(4-0)P(2)	1053.283	11.3
L(4-0)R(3)	1053.9770	13.04
L(4-0)P(3)	1056.4727	10.71
L(6-0)R(3)	1028.9832	22.62
L(7-0)R(1)	1013.43701*	25.8
L(9-0)P(1)	992.8087	37.19
L(9-0)R(0)	991.37891*	32.3
L(9-0)R(1)	992.01637	31.7
L(10-0)P(1)	982.8340	40.53

Table 1: Isolated H_2 Lines Observed in Q0528-250 and Q0347-382

Transition[a]	Rest Wavelength[b] Angstroms	K Factor ($x10^{-3}$)[c]
L(10-0)P(2)	984.86398	31.3
L(10-0)R(1)	982.0728	41.26
L(12-0)R(3)	967.6752	43.86

[a]The nomenclature for the transition is L for Lyman or W for Werner bands, (upper vibrational quantum number - lower vibrational quantum number), R,Q,P transition (lower rotational quantum number).

[b]Wavelengths marked with * indicate wavelengths taken from Ubachs and Reinhold(2004), otherwise from Varshalovich & Potekhin (1995) or Ivanchik et al. 2003.

[c]K factors for Eq. (3 taken from Varshalovich & Potekhin (1995) or Ivanchik et al. 2003.

Table 2: QSOs with known H_2 absorptions

Name	Magnitudes	Absorption Redshifts			
Q0013-004		1.96685	1.96822	1.97296	1.97380
Q0347-383	m_V=17.8	3.02489			
Q0405-443	m_B=17.6	2.59471			
Q0515-441		1.15079			
Q0528-250	m_V=17.24	2.8112			
Q0551-336		1.96168	1.96220		
Q1232+082	m_V=18.4	2.3377			
Q1331+170		1.776553			
Q1444+014	m_B=18.5	2.08680	2.08696		

Figures

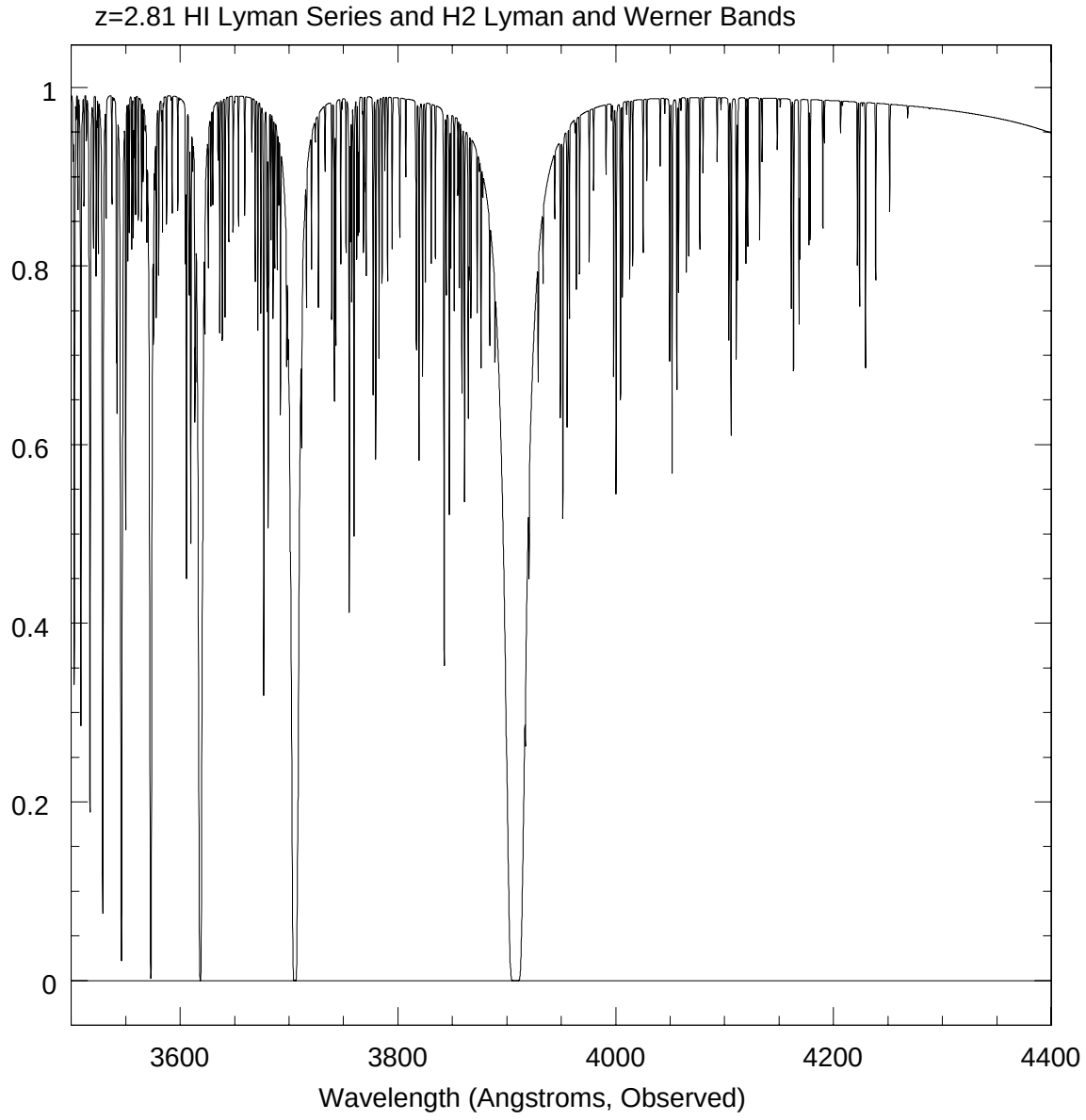

Figure 1. A calculated H_2 spectrum at the redshift (2.81) of the known H_2 absorption system in PKS0528-25. The broad lines are the Ly β, γ etc. lines but all of the rest are due to H_2. Other Ly forest lines are not shown in the system for clarity. Each set of Lyman forest lines acts as a calibrator against which the H_2 line shifts can be calculated. The H_2 with low $\Delta\mu$ shifts also act as calibrators for those with high $\Delta\mu$ shifts.

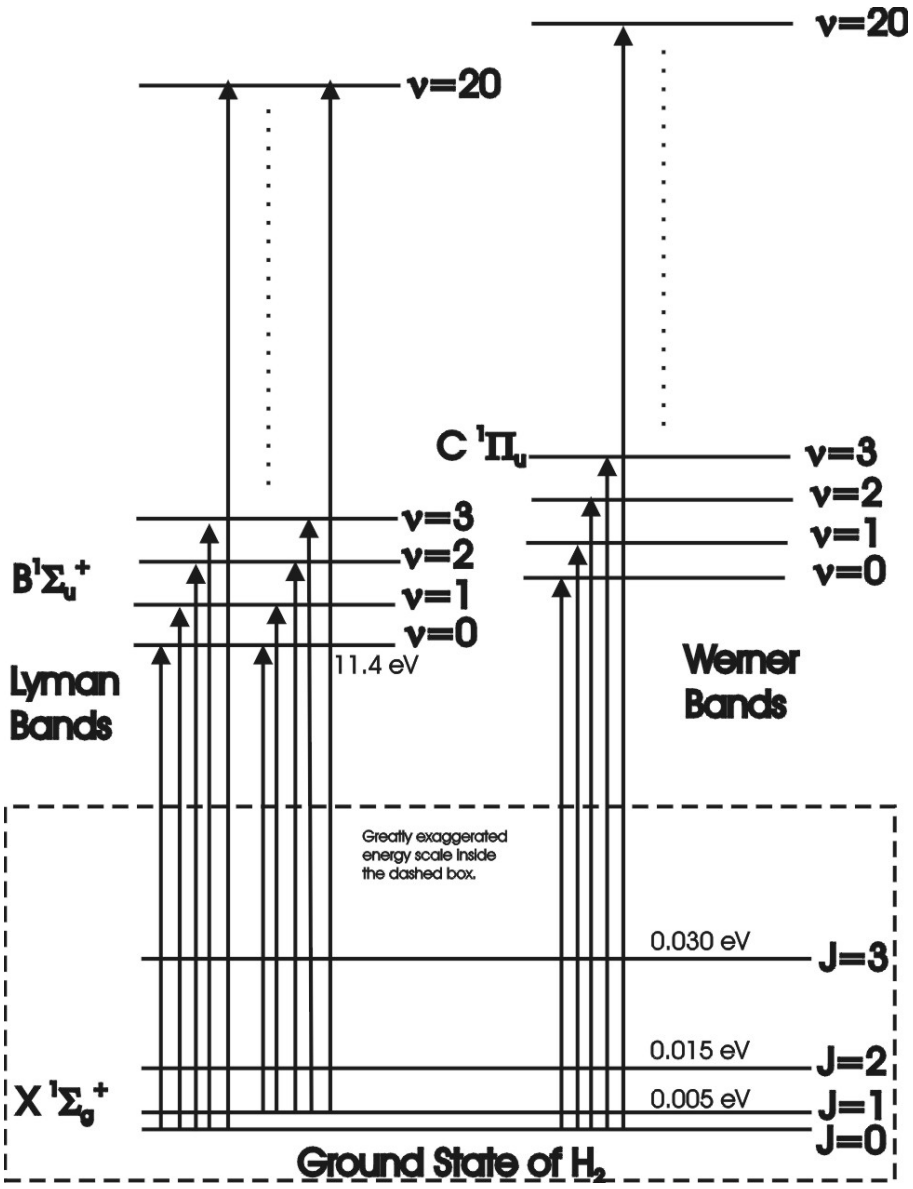

Figure 2. The energy diagram for H_2. The first few rotational levels of the ground electronic and vibrational state are shown at a greatly exaggerated energy scale for clarity (note the energy levels in the box and on the first level of the B Σ state). Only the first few rotational states are populated in the cold H_2 gas of DLAs. Transitions to the upper electronic and vibrational states are shown in the Lyman and Werner bands. The rotational levels of the upper states are suppressed in this diagram. The Lyman band has two branches: R ($J_{upper} = J_{lower}+1$) and P ($J_{upper} = J_{lower}-1$) except for $J_{lower} =0$ which only has the R band. The Werner bands have 3 transitions, R, P and Q ($J_{upper} = J_{lower}$). The figure is schematic only and not to scale.

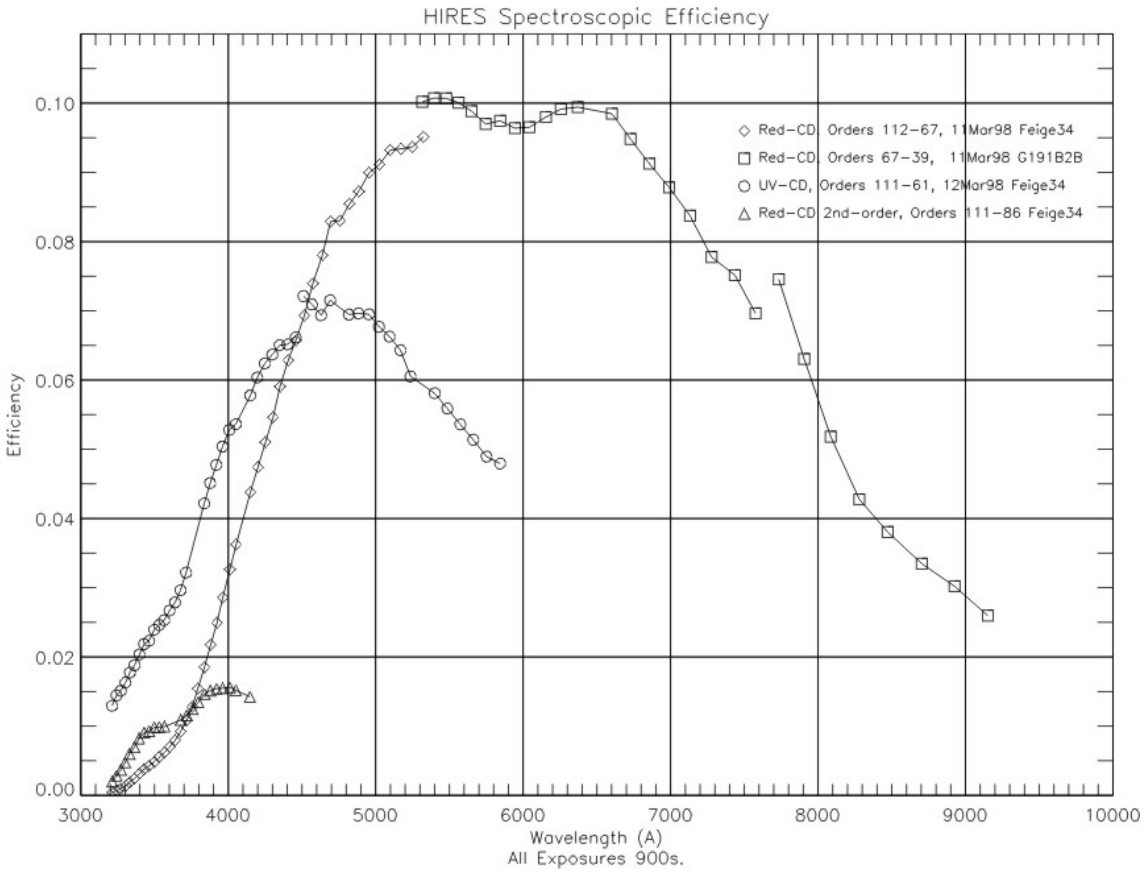

Figure 3. The efficiency of the HIRES spectrometers on the KECK telescope. The plotted efficiency does not included atmospheric transparency, telescope efficiency or slit losses.